Mechanism of the phosphatase component of *Clostridium thermocellum* polynucleotide kinase-phosphatase

NIROSHIKA KEPPETIPOLA and STEWART SHUMAN
Molecular Biology Program, Sloan-Kettering Institute, New York, New York 10021, USA

ABSTRACT

Polynucleotide kinase-phosphatase (Pnkp) from *Clostridium thermocellum* catalyzes ATP-dependent phosphorylation of 5′-OH termini of DNA or RNA polynucleotides and Ni^{2+}/Mn^{2+}-dependent dephosphorylation of 2′,3′ cyclic phosphate, 2′-phosphate, and 3′-phosphate ribonucleotides. *Cth*Pnkp is an 870-amino-acid polypeptide composed of three domains: an N-terminal module similar to bacteriophage T4 polynucleotide kinase, a central module that resembles the dinuclear metallophosphoesterase superfamily, and a C-terminal ligase-like adenylyltransferase domain. Here we conducted a mutational analysis of *Cth*Pnkp that identified 11 residues required for Ni^{2+}-dependent phosphatase activity with 2′-AMP and 3′-AMP. Eight of the 11 *Cth*Pnkp side chains were also required for Ni^{2+}-dependent hydrolysis of *p*-nitrophenyl phosphate. The ensemble of essential side chains includes the conserved counterparts (Asp187, His189, Asp233, Arg237, Asn263, His264, His323, His376, and Asp392 in *Cth*Pnkp) of all of the amino acids that form the dinuclear metal-binding site and the phosphate-binding site of bacteriophage λ phosphatase. Three residues (Asp236, His264, and Arg237) required for activity with 2′-AMP or 3′-AMP were dispensable for Ni^{2+}-dependent hydrolysis of *p*-nitrophenyl phosphate. Our findings, together with available structural information, provide fresh insights to the metallophosphoesterase mechanism, including the roles of His264 and Asp236 in proton donation to the leaving group. Deletion analysis defined an autonomous phosphatase domain, *Cth*Pnkp-(171–424).

Keywords: RNA/DNA end-healing; phosphoesterase; dinuclear metal cluster; λ phosphatase

INTRODUCTION

When breakage of a 3′-5′ phosphodiester in DNA or RNA results in the formation of 5′-OH and 3′-PO_4 (or 2′,3′ cyclic PO_4) termini, the broken ends must be "healed" before they can be sealed by polynucleotide ligase. Healing occurs via hydrolysis of the 3′-PO_4 (or 2′,3′ cyclic phosphate) to form a 3′-OH and phosphorylation of the 5′-OH to form a 5′-PO_4 end. Bacteriophage T4 polynucleotide 5′-kinase/3′-phosphatase (Pnkp) is the prototypal end-healing enzyme (Richardson 1965; Novogrodsky and Hurwitz 1966; Novogrodsky et al. 1966; Cameron and Uhlenbeck 1977; Amitsur et al. 1987; Wang and Shuman 2001, 2002; Wang et al. 2002; Galburt et al. 2002). Additional Pnkp enzymes have been identified and characterized from other bacteriophages, eukarya, and a eukaryotic virus (Martins and Shuman 2004; Zhu et al. 2004; Bernstein et al. 2005; Blondal et al. 2005), but only recently has an end-healing activity been discovered in a bacterial proteome—that of the anaerobic thermophile *Clostridium thermocellum* (Martins and Shuman 2005).

*Cth*Pnkp catalyzes the phosphorylation of 5′-OH termini of DNA or RNA polynucleotides and the dephosphorylation of 2′,3′ cyclic phosphate, 2′-phosphate, and 3′-phosphate ribonucleotides. *Cth*Pnkp also catalyzes an autoadenylylation reaction via a polynucleotide ligase-type mechanism. These characteristics are consistent with a role in end-healing during RNA or DNA repair. *Cth*Pnkp is a homodimer of an 870-amino-acid polypeptide composed of three catalytic domains: an N-terminal module that resembles the polynucleotide kinase domain of bacteriophage T4 Pnkp, a central metal-dependent phosphoesterase module, and a C-terminal module that resembles the nucleotidyl transferase domain of polynucleotide ligases (Fig. 1). Putative trifunctional homologs of *Cth*Pnkp are encoded by several other bacterial genera, including *Kinetococcus*, *Nostoc*, *Streptomyces*, *Fusobacterium*, *Bacillus*, and

Reprint requests to: Stewart Shuman, Molecular Biology Program, Sloan-Kettering Institute, 1275 York Avenue, New York, NY 10021, USA; e-mail: s-shuman@ski.mskcc.org; fax: (212) 717-3623.

Article published online ahead of print. Article and publication date are at http://www.rnajournal.org/cgi/doi/10.1261/rna.2196406.

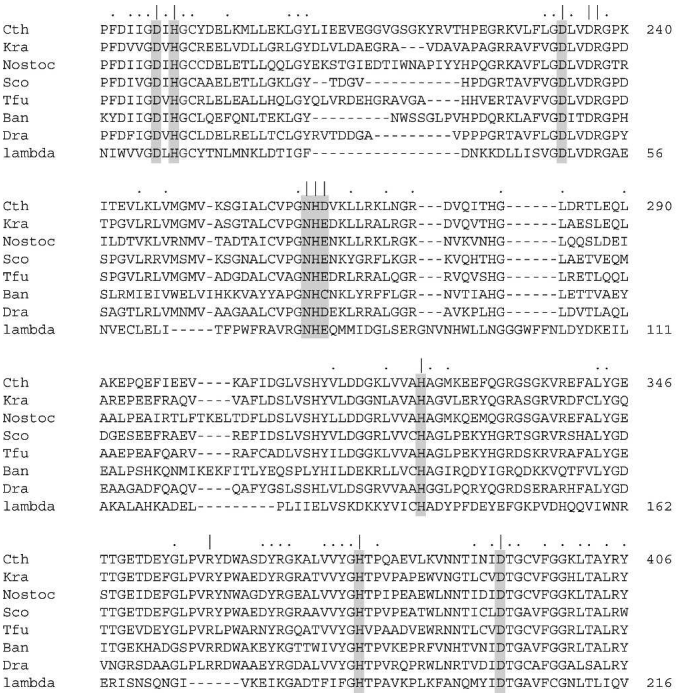

Cth	lambda	Contacts
Asp187	Asp20	Manganese 1
His189	His22	Manganese 1
Asp233	Asp49	Manganese 1 and 2
Asp236	Asp52	His76, Trp93
Arg237	Arg53	Sulfate
Asn263	Asn75	Manganese 2 / Sulfate
His264	His76	Sulfate, Asp52
Asp265	Glu77	Asp49 N, Leu50 N, Gly74 N
His323	His139	Manganese 2
Arg359	-	-
His376	His186	Manganese 2
Asp392	Asp202	HOH to Manganese 1

FIGURE 1. The phosphoesterase domain of *Cth*Pnkp. (*Left*) The amino acid sequence of *Cth*Pnkp(172–406) is aligned to the sequences of homologous proteins of *Kineococcus radiotolerans*, *Nostoc sp. PCC 7120*, *Streptomyces coelicolor*, *Thermobifida fusca*, *Bacillus anthracis*, *Deinococcus radiodurans*, and bacteriophage λ. Gaps in the alignment are indicated by dashes. The amino acids subjected to mutational analysis in the present study are indicated by |. The side chains that bind a dinuclear metal cluster and coordinate the phosphate in the active site in the crystal structure of λ phosphatase are highlighted in shaded boxes. Other positions of amino acid side chain identity or similarity in all proteins are indicated by dots *above* the alignment. (*Right*) The mutated amino acids of *Cth*Pnkp are listed *next* to their counterparts in λ phosphatase and the atomic contacts of these side chains in the crystal structure of λ phosphatase.

Helicobacter (Martins and Shuman 2005). Putative bifunctional Pnkp homologs in *Deinococcus* and *Thermobifida* are composed only of the kinase and the phosphoesterase domain equivalents of *Cth*Pnkp, with no equivalent of the adenylyltransferase domain.

The distinctive feature of *Cth*Pnkp and its relatives vis-à-vis known RNA/DNA repair enzymes is that its 3′ end-modification component belongs to the calcineurin-type metallophosphoesterase superfamily (Goldberg et al. 1995; Rusnak and Mertz 2000). It contains putative counterparts of the amino acids that form the dinuclear metal-binding site and the phosphate-binding site of bacteriophage λ phosphatase (Voegtli et al. 2000). As with λ phosphatase (Zhuo et al. 1993), the 2′,3′ cAMP phosphatase activity of *Cth*Pnkp is specifically dependent on either nickel (Ni) or manganese. Here we address the following questions: (1) Is the primary structure similarity between *Cth*Pnkp and λ phosphatase functionally relevant? (2) If so, what features of the conserved side chains are essential for activity? (3) How do structure–function relationships illuminate the reaction mechanism? (4) Is phosphohydrolase activity restricted to nucleotide substrates? (5) Are the kinase and adenylyltransferase domains required for phosphatase activity, or does the phosphatase function reside within an autonomous domain of the *Cth*Pnkp protein?

RESULTS

Alanine scanning identifies the phosphoesterase active site of *Cth*Pnkp

The amino acid sequence of the central phosphatase-like domain of *C. thermocellum* Pnkp is shown in Figure 1, aligned to the sequences of homologous proteins of *Kineococcus radiotolerans*, *Nostoc sp. PCC 7120*, *Streptomyces coelicolor*, *Thermobifida fusca*, *Bacillus anthracis*, and *Deinococcus radiodurans*, and to the phosphoprotein phosphatase of bacteriophage λ. The alignment highlights the fact that *Cth*Pnkp and its bacterial homologs contain the full constellation of conserved residues that bind a dinuclear metal cluster and coordinate a sulfate in the active site in the crystal structure of λ phosphatase (Fig. 2; Voegtli et al. 2000). To probe the mechanistic and structural relatedness of *Cth*Pnkp and λ phosphatase, we introduced single alanine mutations at 12 positions within the full-length *Cth*Pnkp polypeptide, 11 of which (Asp187, His189, Asp233, Asp236, Arg237, Asn263, His264, Asp265, His323, His376, Asp392) are conserved in the bacterial homologs and λ phosphatase. The other targeted residue, Arg359, is conserved in the bacterial proteins but is apparently missing from λ phosphatase (Fig. 1).

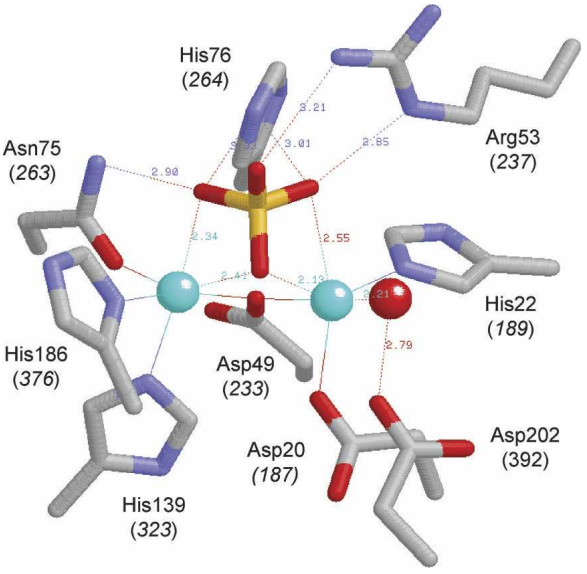

FIGURE 2. The active site of λ phosphatase. The figure depicts the active site of the manganese- and sulfate-bound λ phosphatase (molecule C) from the crystal structure of Voegtli et al. (2000; Protein Data Bank 1G5B). The amino acid side chains coordinating the binuclear metal cluster and the sulfate ion are shown. The corresponding amino acids of *Cth*Pnkp are indicated in parentheses. The manganese ions are colored cyan. Water is colored red. The structure is predicted to mimic the product (P_i) complex of the enzyme.

The *Cth*Pnkp-Ala mutants were produced in *Escherichia coli* as His_{10}-tagged fusions in parallel with the wild-type protein and then purified from soluble bacterial extracts by adsorption to Ni-agarose and elution with buffer containing imidazole. SDS-PAGE analysis showed that the protein preparations consisted principally of a ~100-kDa polypeptide corresponding to His_{10}-*Cth*Pnkp (Fig. 3A). Minor polypeptides of 45 and 55 kDa likely corresponded to proteolytic fragments of *Cth*Pnkp (see below). The recombinant wild-type Pnkp catalyzed phosphate release from either 2′-AMP or 3′-AMP in the presence of $NiCl_2$ (Fig. 3B,C). Eleven of the alanine mutations either abolished or severely diminished phosphatase activity with 2′-AMP and 3′-AMP substrates. Our operational definition of a significant mutational effect is one that reduces activity to <20% of the wild-type value. The 11 residues defined by the alanine scan as essential or important for phosphatase function correspond to those that are conserved in λ phosphatase (Fig. 1). In contrast, the R359A mutation had little effect on hydrolysis of 3′-AMP (Fig. 3C) and only a modest impact on hydrolysis on 2′-AMP (Fig. 3B) that did not meet our criterion for functional importance. All of the Pnkp-Ala proteins retained polynucleotide kinase activity, measured by transfer of $^{32}P_i$ from [γ-^{32}P]ATP to the 5′-OH terminus of an 36-mer oligodeoxyribonucleotide to form a 5′ ^{32}P-labeled oligonucleotide product (data not shown), signifying that the observed mutational effects on phosphatase function were probably not caused by global effects on protein folding. These results suggest that the phosphatase component of *Cth*Pnkp has an active site similar to that of λ phosphatase.

Hydrolysis of a non-nucleotide phosphomonoester substrate

Although the linkage of the *Clostridium* 2′,3′-phosphatase to a polynucleotide kinase domain and a ligase-like adenylyltransferase domain suggested a role in nucleic acid repair, the reports that λ-like phosphatases are able to hydrolyze non-nucleotide and nonprotein phosphate-containing substrates (Zhuo et al. 1993; Mertz et al. 1997; Chen et al. 2004; Schenk et al. 2005) prompted us to test the activity of *Cth*Pnkp with the generic substrate *p*-nitrophenyl phosphate. We found that the enzyme readily converted *p*-nitrophenyl phosphate (10 mM) to *p*-nitrophenol in the presence of 10 mM $NiCl_2$. The rate and extent of product formation was proportional to input *Cth*Pnkp (Fig. 4A). Hydrolysis of 10 mM *p*-nitrophenyl phosphate was optimal at 2–10 mM Ni; activity at 0.5 mM Ni was 77% of the optimum value (data not shown). Magnesium, copper, cadmium calcium, or zinc (at 10 mM concentration) could not satisfy the divalent cation requirement (not shown). A mixing experiment was performed in which reactions containing 10 mM Ni were supplemented with 10 mM of each of the other divalent cations. Whereas magnesium and calcium neither significantly stimulated nor inhibited the hydrolysis of *p*-nitrophenyl phosphate, activity was abolished in the presence of copper, cadmium, or zinc (data not shown).

Our initial tests of manganese as a cofactor indicated that mixtures containing 10 mM *p*-nitrophenyl phosphate and manganese resulted in enzyme-independent generation of a brown-colored solution after the reactions were quenched with sodium carbonate, which caused a significant enzyme-independent background of absorbance at 410 nm. The background was absent at 0.5 mM manganese, increased linearly from 1–3 mM manganese, and plateaued at ≥5 mM. Whereas mixing 10 mM cobalt with 10 mM *p*-nitrophenyl phosphate also generated a light brown color, this background was absent at 0.5 mM cobalt. To avoid these background complications, we reassayed the hydrolysis of *p*-nitrophenyl phosphate in the presence of 0.5 mM divalent cations. Ni and manganese supported similar levels of phosphatase activity, whereas cobalt was ~20% as effective (Fig. 4B). Magnesium, calcium copper, cadmium, and zinc were ineffective. The selectivity for Ni and manganese in hydrolysis of *p*-nitrophenyl phosphate mirrors the requirements for hydrolysis of 2′,3′ cyclic AMP, 2′-AMP, and 3′-AMP substrates reported previously (Martins and Shuman 2005). When the metal mixing experiment was performed at 0.5 mM Ni and 0.5 mM of the second metal, we found that: (1) manganese did not synergize with Ni; (2) magnesium and calcium had little effect; (3) cobalt reduced activity to a level comparable to that of cobalt alone; and (4) copper, cadmium, and zinc were more strongly inhibitory. A simple

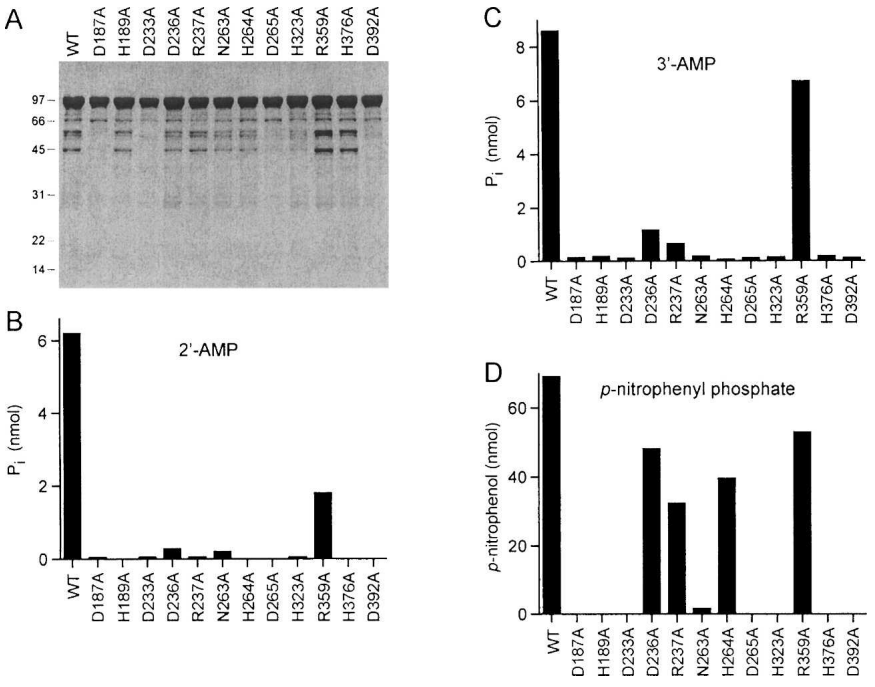

FIGURE 3. Effects of alanine mutations on *Cth*Pnkp phosphatase activity. (*A*) Aliquots (5 μg) of the Ni-agarose preparations of the wild-type (WT) and Ala-mutant *Cth*Pnkp were analyzed by SDS-PAGE. The Coomassie blue-stained gel is shown. The positions and sizes (kDa) of marker polypeptides are indicated on the *left*. (*B*) Reaction mixtures (25 μL) containing 50 mM Tris-HCl (pH 7.5), 5 mM $NiCl_2$, 5 mM 2′-AMP, and 0.5 μg wild-type or mutant *Cth*Pnkp were incubated for 30 min at 45°C. (*C*) Reactions mixture (25 μL) containing 50 mM Tris-HCl (pH 7.5), 5 mM $NiCl_2$, 5 mM 3′-AMP, and 1 μg *Cth*Pnkp were incubated for 30 min at 45°C. (*D*) Reaction mixtures (25 μL) containing 50 mM Tris-HCl (pH 7.5), 10 mM $NiCl_2$, 10 mM *p*-nitrophenyl phosphate, and 0.5 μg *Cth*Pnkp were incubated for 30 min at 45°C.

interpretation of these results is that copper, cobalt, cadmium, and zinc compete with Ni for one or both sites in the binuclear metal cluster to generate a catalytically inert or impaired metalloenzyme, whereas magnesium and calcium do not compete well with Ni for the metal-binding sites.

Distinctive effects of alanine mutations on hydrolysis of *p*-nitrophenyl phosphate

Eight of the alanine mutations of *Cth*Pnkp either abolished or severely diminished phosphatase activity with *p*-nitrophenyl phosphate as the substrate (Fig. 3D). The residues thereby defined as essential for production of *p*-nitrophenol include all of the predicted direct or water-mediated ligands of the binuclear metal cluster (Asp187, His189, Asp233, Asn263, His323, His376, Asp392) (Figs. 1, 2), signifying that the same mechanism of metal-dependent catalysis is employed by *Cth*Pnkp with nucleotide and non-nucleotide substrates. Mutation of Arg359 had little impact on hydrolysis of *p*-nitrophenyl phosphate (Fig. 3D), which was consistent with the results for the nucleotide substrates. The interesting findings were that Asp236, Arg237, and His264 were not required for hydrolysis of *p*-nitrophenyl phosphate, although they clearly were critical for activity with 2′-AMP and 3′-AMP (Fig. 3). We discuss these results below in the context of a model of general acid catalysis involving Asp236 and His264, whereby the requirement for proton donation is alleviated for hydrolysis of *p*-nitrophenyl phosphate by the low pK_a of the *p*-nitrophenol leaving group.

Structure–function relationships at essential residues

Conservative substitutions were introduced at the 11 positions defined by the alanine scan as essential/important for phosphatase activity with the 2′-AMP or 3′-AMP substrates. Aspartate was replaced by glutamate and asparagine, histidine by asparagine and glutamine, arginine by lysine and glutamine, and asparagine by aspartate and glutamine. The 22 conservative mutants were produced in *E. coli* as His_{10}-tagged fusions and purified from soluble extracts by Ni-agarose chromatography, in parallel with the wild-type *Cth*Pnkp (Fig. 5A). The effects

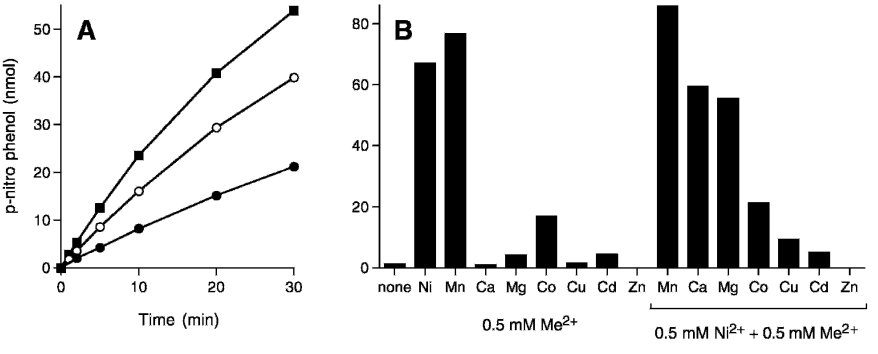

FIGURE 4. Hydrolysis of *p*-nitrophenyl phosphate. (*A*) Kinetics. Reaction mixtures (200 μL) containing 50 mM Tris-HCl (pH 7.5), 10 mM $NiCl_2$, 10 mM *p*-nitrophenyl phosphate, and either 1 μg (●), 2 μg (○), or 4 μg (■) of *Cth*Pnkp were incubated at 45°C. Aliquots (25 μL) were withdrawn at the times specified and quenched immediately with sodium carbonate. *p*-Nitrophenol formation is plotted as a function of time. (*B*) Metal-specificity. Reaction mixtures (25 μL) contained 50 mM Tris-HCl (pH 7.5), 10 mM *p*-nitrophenyl phosphate, 1 μg *Cth*Pnkp, and either no divalent cation (none), 0.5 mM of the indicated divalent metal (Me^{2+}) alone, or 0.5 mM $NiCl_2$ plus 0.5 mM of the indicated divalent metal. All metals were added as the chloride salt. Reactions were incubated for 30 min at 45°C.

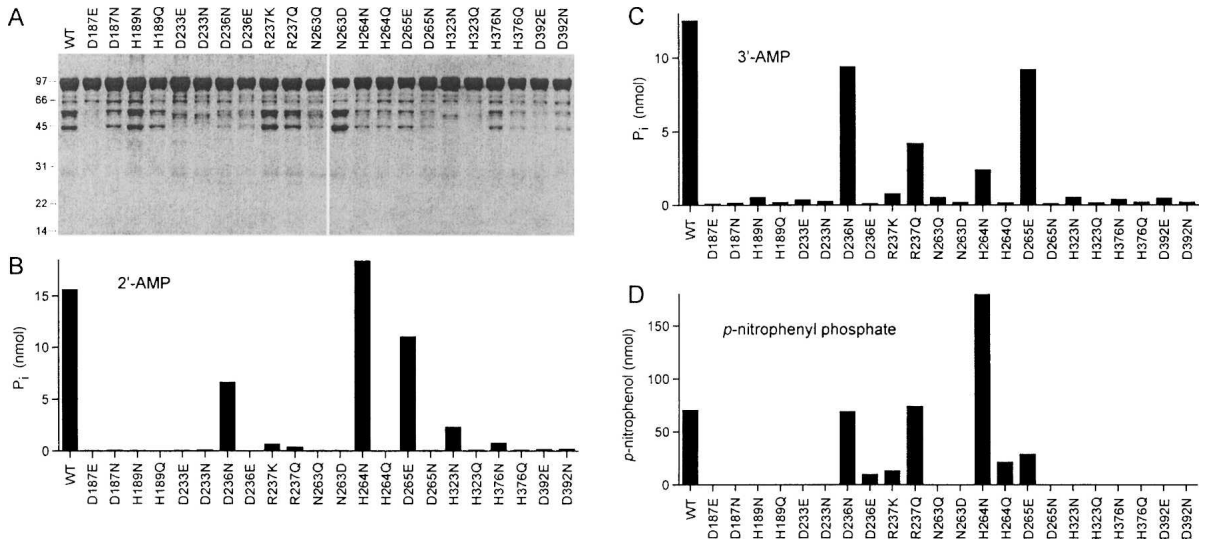

FIGURE 5. Effects of conservative mutations on *Cth*Pnkp phosphatase activity. (*A*) Aliquots (5 μg) of the Ni-agarose preparations of wild-type (WT) *Cth*Pnkp and conservative mutants were analyzed by SDS-PAGE. The Coomassie blue-stained gel is shown. The positions and sizes (kDa) of marker polypeptides are indicated on the *left*. (*B*) Reaction mixtures (25 μL) containing 50 mM Tris-HCl (pH 7.5), 5 mM $NiCl_2$, 5 mM 2′-AMP, and 1 μg *Cth*Pnkp as specified were incubated for 30 min at 45°C. (*C*) Reactions mixture (25 μL) containing 50 mM Tris-HCl (pH 7.5), 5 mM $NiCl_2$, 5 mM 3′-AMP, and 1 μg *Cth*Pnkp as specified were incubated for 30 min at 45°C. (*D*) Reaction mixtures (25 μL) containing 50 mM Tris-HCl (pH 7.5), 10 mM $NiCl_2$, 10 mM *p*-nitrophenyl phosphate, and 0.5 μg *Cth*Pnkp as specified were incubated for 30 min at 45°C.

of the mutations on the release of P_i from 2′-AMP and 3′-AMP substrates are shown in Figure 5, B and C, respectively. Effects on the release of *p*-nitrophenol from *p*-nitrophenyl phosphate are shown in Figure 5D. The notable finding was that all seven side chains predicted to make direct or water-mediated contacts to the binuclear metal cluster (Asp187, His189, Asp233, Asn263, His323, His376, Asp392) were strictly essential for phosphatase activity with all three substrates; i.e., both of the conservative substitutions tested at each position either abolished or significantly suppressed product formation. These results attest to the lack of plasticity in the metal-binding site of *Cth*Pnkp.

Conservative substitutions at other positions resulted in significant gains of function compared with an alanine mutant. For example, whereas D265A was virtually inert with all substrates, introduction of a glutamate restored activity to 70%, 74%, and 39% of the wild-type value with 2′-AMP, 3′-AMP, and *p*-nitrophenyl phosphate, respectively (Fig. 5). In contrast, the conservative D265N change had no salutary effect. These results signify that a carboxylate functional group is critical at position 265. Note that this position is naturally occupied by glutamate (Glu77) in λ phosphatase and several bacterial homologs of *Cth*Pnkp (Fig. 1). The Glu77 side chain in λ phosphatase makes no contacts with either the metal cluster or the sulfate ion (a mimetic of phosphate) but rather appears to play a structural role in ensuring the proper conformation of the active site, via hydrogen bonds from the glutamate to three backbone amide nitrogens, including that of Asp49 (Asp233 in *Cth*Pnkp) (Fig. 1), which coordinates both of the divalent cations (Fig. 2).

The R237A change suppressed hydrolysis of 2′-AMP and 3′-AMP, but not *p*-nitrophenyl phosphate. Whereas the conservative R237Q mutant was as active as the wild-type enzyme with *p*-nitrophenyl phosphate (Fig. 5D) and 34% as active as the wild-type with 3′-AMP (Fig. 5C), there was no gain of function in hydrolysis of 2′-AMP (Fig. 5B). Note that the conservative R237K mutant was as defective as R237A with 2′-AMP or 3′-AMP and was even more defective than was R237A with *p*-nitrophenyl phosphate (Fig. 5). These results show that (1) the requirement for Arg237 is substrate dependent; (2) a positive charge is not sufficient for optimal activity with any substrate tested, i.e., lysine is detrimental in lieu of arginine; and (3) hydrogen bonding capacity is probably the critical property for activity with 3′-AMP, insofar as glutamine elicited a gain of function. The crystal structure of λ phosphatase shows that the equivalent of Arg237 makes a bidentate contact with a sulfate ion that likely mimics the phosphate of the product complex (Fig. 2).

H264A also blocked hydrolysis of 2′-AMP and 3′-AMP, but not *p*-nitrophenyl phosphate. Replacement by asparagine restored hydrolysis of 2′-AMP and 3′-AMP to 118% and 19% of the wild-type levels, respectively, but glutamine had no salutary effect (Fig. 5B,C). It is notable that the activity of the H264N protein with *p*-nitrophenyl phosphate was several fold higher than that of wild-type *Cth*Pnkp, whereas H264Q was 31% as active as wild type (Fig. 5D). The crystal structure of λ phosphatase shows that the histidine equivalent to His264 of *Cth*Pnkp coordinates the sulfate ion via Nε (Fig. 2), while Nδ makes a hydrogen bond to the aspartate side chain corresponding to Asp236 of *Cth*Pnkp (Fig. 1). It is therefore surprising that replacing

His264 with asparagine, which mimics the Nδ functional group of histidine, results in much higher activity than does glutamine, which mimics the Nε functional group. As discussed below, these results have mechanistic implications concerning models of general acid catalysis by members of the calcineurin-like superfamily (Rusnak and Mertz 2000; Hopfner et al. 2001).

D236A suppressed activity with 2′-AMP and 3′-AMP, but not with *p*-nitrophenyl phosphate. Asparagine restored activity to 42% and 75% of the wild-type levels with 2′-AMP, 3′-AMP, respectively, and supported full activity with *p*-nitrophenyl phosphate. In contrast, glutamate abolished activity with 2′-AMP and 3′-AMP and reduced activity with *p*-nitrophenyl phosphate to 14% of the wild-type level. The finding that an isosteric amide is functional in lieu of the carboxylate implies that hydrogen bonding capacity (presumably to Nδ of His264; see above) is the relevant characteristic of this side chain in promoting hydrolysis of nucleotide phosphomonoesters. We infer a tight steric constraint on this side chain, insofar as the extra methylene group of glutamate was detrimental to catalysis.

Effects of selected mutations on K_m and k_{cat}

We determined steady-state kinetic parameters for hydrolysis of *p*-nitrophenyl phosphate at pH 7.5 in the presence of 10 mM Ni. Formation of *p*-nitrophenol by *Cth*Pnkp displayed a hyperbolic dependence on the concentration of the *p*-nitrophenyl phosphate substrate (data not shown). From a double reciprocal plot, we calculated a K_m value of 2.5 mM and a k_{cat} of 818 min^{-1} (Table 1). Kinetic parameters were then determined for the set of nine proteins mutated at residues Asp236, Arg237, and His264 (Table 1). The k_{cat} values for D236A (512 min^{-1}), R237A (352 min^{-1}) and H264A (402 min^{-1}) confirmed the inferences from single-point assays that none of the three side chains is important for the chemistry of *p*-nitrophenyl phosphate hydrolysis. The K_m values of the three alanine mutants were similar (within a factor of two) to that of wild-type *Cth*Pnkp. Notable findings were that the conservative H264N mutation resulted in a eightfold increase in k_{cat} (to 6770 min^{-1}) relative to wild-type enzyme, without significantly affecting the K_m for *p*-nitrophenyl phosphate, whereas the turnover number of the H264Q protein was about half that of H264A (Table 1). Grossly disparate effects of conservative replacements on kinetic parameters were also seen at Arg237, where lysine preserved substrate binding but reduced k_{cat} to 108 min^{-1}, whereas glutamine lowered the substrate affinity several-fold (K_m 8.6 mM) but increased k_{cat} slightly (to 1090 min^{-1}) compared with wild-type *Cth*Pnkp.

TABLE 1. Kinetic parameters for hydrolysis of *p*-nitrophenyl phosphate

Protein	K_m (mM)	k_{cat} (min^{-1})
Wild-type	2.5 ± 0.7	818 ± 77
D236A	1.3 ± 0.4	512 ± 81
D236N	0.85 ± 0.05	762 ± 21
D236E	2.5 ± 0.6	146 ± 2
R237A	4.0 ± 0.05	352 ± 30
R237K	3.2 ± 0.05	108 ± 7
R237Q	8.6 ± 1.1	1090 ± 48
H264A	1.7 ± 0.1	402 ± 42
H264N	3.8 ±1.2	6770 ± 1430
H264Q	2.8 ± 0.4	228 ± 39

Reaction mixtures (25 μL) containing 50 mM Tris-HCl (pH 7.5); 10 mM $NiCl_2$; 0, 0.625, 1.25, 2.5, 5, 10, or 15 mM *p*-nitrophenyl phosphate; and a fixed amount (between 0.25 and 1 μg) of one of the indicated *Cth*Pnkp proteins were incubated for 15 min at 45°C. *p*-Nitrophenol production was plotted as a function of substrate concentration, and then K_m and k_{cat} values were calculated from double-reciprocal plots of the data. The values in the table are averages from two independent substrate titration experiments.

An autonomous phosphatase domain of *Cth*Pnkp

We produced recombinant His_{10}-tagged versions of three N-terminal deletion mutants: *Cth*Pnkp-(125–870), *Cth*Pnkp-(159–870), and *Cth*Pnkp-(171–870). The truncated proteins were purified from soluble *E. coli* extracts by Ni-agarose chromatography and displayed the expected decrements in electrophoretic mobility compared with the full-length protein (Fig. 6A). Whereas the ~55-kDa contaminant was present in all of the preparations, the ~45-kDa contaminant seen in the wild-type enzyme was absent in the truncated protein preparations, being replaced by a set of discrete lower-molecular-weight contaminants with mobility differences that correspond to the differences in their respective N termini (Fig. 6A). This pattern suggests that the ~55-kDa contaminant is a C-terminal proteolytic fragment of *Cth*Pnkp, whereas the smaller polypeptides are proteolytic fragments derived from the upstream segment of the recombinant protein. All three N-terminal deletion mutants retained phosphatase activity with either 2′-AMP or 3′-AMP substrates (Fig. 6B) but were inert with respect to 5′ polynucleotide kinase activity (data not shown). Thus, an upstream margin of the phosphatase domain (amino acid 171) is positioned only 17 amino acids upstream of essential residue Asp187 identified in the alanine scan.

To test if the C-terminal adenylyltransferase domain of *Cth*Pnkp plays a role in the phosphatase reaction, we produced two other series of deletion mutants with N termini fixed at either residue 159 or 171 (based on the results in Fig. 6B) and C termini at residues 472, 444, or 424. The six truncated proteins were purified from soluble *E. coli* extracts by Ni-agarose chromatography and displayed the expected variations in electrophoretic mobility (Fig. 6C). The pattern of minor polypeptide fragments—comprising a 30-kDa species when the N terminus was at residue 159 and a 28-kDa species when the N terminus was at residue 171—suggested that the proteins underwent proteolytic cleavage at a single discrete site located near the C termini of all of

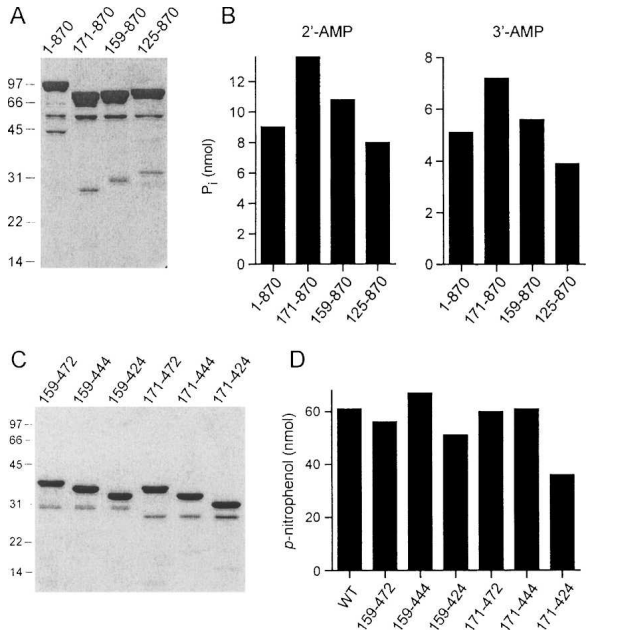

FIGURE 6. N-terminal and C-terminal deletions. Aliquots (5 μg) of the Ni-agarose preparations of the wild-type (WT) *Cth*Pnkp and the indicated N-terminal deletion mutants (*A*) or C-terminal truncation mutants (*C*) were analyzed by SDS-PAGE. The Coomassie blue-stained gels are shown. The positions and sizes (kDa) of marker polypeptides are indicated on the *left*. (*B*) Reactions mixtures (25 μL) containing 50 mM Tris-HCl (pH 7.5), 10 mM $NiCl_2$, 1 μg *Cth*Pnkp as specified, and 5 mM 2′-AMP or 3′-AMP were incubated for 30 min at 45°C. (*D*) Reactions mixtures (25 μL) containing 50 mM Tris-HCl (pH 7.5), 10 mM $NiCl_2$, 10 mM *p*-nitrophenyl phosphate, and 10 pmol of enzyme as specified were incubated for 30 min at 45°C.

the proteins. The truncated proteins were tested for hydrolysis of *p*-nitrophenyl phosphate in parallel with wild-type *Cth*Pnkp; because the wild-type and truncated proteins differed in size, the input protein in the assay was adjusted to attain approximately equimolar enzyme. The deletion of protein distal to residues 472 or 444 had no apparent impact on activity (Fig. 6D), whereas further truncation of the C terminus to residue 424 (located just 32 amino acids downstream of essential residue Asp392) had only a modest effect (Fig. 6D). As the proteins in this series lacked the adenylyltransferase domain, we surmise that it plays no role in the phosphatase activity. We conclude that the phosphatase resides within an autonomous central domain of *Cth*Pnkp located between residues 171 and 424. Shorter truncation mutants were not tested.

DISCUSSION

Here we conducted a structure–function analysis of the phosphatase domain of *Cth*Pnkp, guided by its amino acid sequence similarity to λ phosphatase and other members of the metallophosphoesterase superfamily. The alanine scan pinpointed 11 residues required for hydrolysis of 2′-AMP and 3′-AMP that are conserved in several bacterial homologs of *Cth*Pnkp and in λ phosphatase. Eight of these side chains are also essential for hydrolysis of the non-nucleotide substrate *p*-nitrophenyl phosphate. Structure–activity relationships were clarified by conservative substitutions. Our results can be interpreted in light of structural information available for λ phosphatase (Voegtli et al. 2000), which shares with *Cth*Pnkp a requirement for either Ni or manganese, and for *Pyrococcus furiosus* Mre11 (Hopfner et al. 2001), a manganese-dependent DNA phosphodiesterase. The findings provide fresh insights to the metallophosphoesterase catalytic mechanism.

The active sites of λ phosphatase (Fig. 2) and *Pfu*Mre11 (Fig. 7) contain two manganese ions coordinated directly or via water by aspartate, histidine, and asparagine side chains. The metal ligands in λ phosphatase are strictly conserved in *Cth*Pnkp. In *Pfu*Mre11, the water-to-Asp constituent of the octahedral complex of one of the manganese ions is replaced by a direct contact to a histidine side chain (Fig. 7). The λ phosphatase structure contains a sulfate ion in a position that is proposed to mimic the product complex of the enzyme with phosphate. The *Pfu*Mre11 structure contains 5′-dAMP and can be viewed as a substrate complex for reasons discussed below. The mechanism of the phosphatase reaction is somewhat controversial, insofar as there are divergent models in the literature concerning the identity of the nucleophilic water, the expulsion of the leaving group, and the nature of the transition state (Rusnak and Mertz

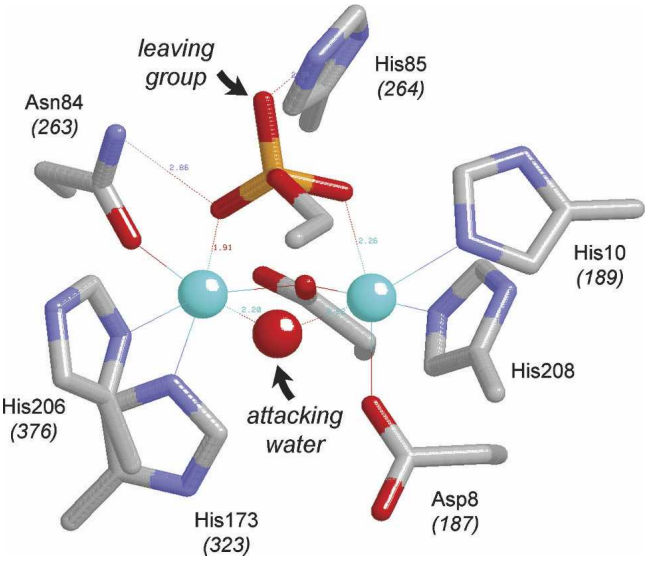

FIGURE 7. The active site of *Pfu*Mre11. The figure depicts the active site of the manganese- and 5′-dAMP-bound *P. furiosus* phosphodiesterase Mre11 from the crystal structure of Hopfner et al. (2001) (Protein Data Bank 1II7). The amino acid side chains coordinating the binuclear metal cluster and the nucleotide 5′ phosphate are shown. The corresponding amino acids of *Cth*Pnkp are indicated in parentheses. The manganese ions are colored cyan. Water is colored red. The structure is predicted to mimic the substrate complex of the enzyme. The proposed nucleophilic water and the phosphate oxygen corresponding to the 3′-O leaving group are indicated. For simplicity, only the phosphate and the ribose O5 and C5 atoms of the nucleotide are shown.

2000; Voegtli et al. 2000; Hopfner et al. 2001). We favor the view that the bridging water between the two manganese ions seen in the *Pfu*Mre11 structure is the attacking nucleophile, because it is located 3.1 Å from the phosphorus atom and is almost perfectly apical to the phosphate oxygen atom of the leaving group, which is a nucleoside 3′-O in the case of Mre11 (Fig. 7). As discussed by Voegtli et al. (2000), the bridging water ligand between the manganese ions should have a low pK_a and thereby be activated by the metals for attack on the phosphate. Comparison of the *Pfu*Mre11 substrate complex in Figure 7 with the λ phosphatase product complex in Figure 2 suggests that the attacking hydroxyl nucleophile becomes incorporated into the phosphate product and continues to occupy the bridging position between the two metal ions; moreover, there is an apparent stereochemical inversion of the phosphorus center, as expected for the in-line single displacement mechanism proposed for the metallophosphoesterases (Mueller et al. 1993). In addition to activating the nucleophile, the metals directly coordinate two nonbridging phosphate oxygens.

We show here that every one of the seven side chains that comprise the metal-binding site of λ phosphatase is strictly essential for *Cth*Pnkp phosphatase activity with all substrates tested; not even conservative substitutions are tolerated at Asp187, His189, Asp233, Asn263, His323, His376, and Asp392. Mutational studies of λ phosphatase had established essential catalytic roles for five metal-binding residues: Asp20, His22, Asp49, Asn75, and His186 (Zhuo et al. 1994; White et al. 2001), which are equivalent to Asp187, His189, Asp233, Asn263, and His376 of *Cth*Pnkp. Of particular interest is the essential Asn263 side chain of *Cth*Pnkp, which is consistently seen to make contacts to both manganese (via Oδ) and one of the phosphate oxygens (via Nδ) (Figs. 2, 7). Our results indicate that both atomic contacts are required for activity.

We obtained additional functional insights to the reaction mechanism via the substrate-specific effects of mutations at Asp236, His264, and Arg237 of *Cth*Pnkp, whereby these residues are required for activity with 2′-AMP and 3′-AMP but not with *p*-nitrophenyl phosphate. His264 coordinates two phosphate oxygens in the λ phosphatase and *Pfu*Mre11 crystal structures; in the *Pfu*Mre11 substrate complex, it donates a hydrogen bond from Nε to the leaving group oxygen (Fig. 7). It has been suggested that this histidine could serve as a general acid catalyst, by donating a proton to the leaving group (Rusnak and Mertz 2000; Hopfner et al. 2001). The preservation of function of the H264A mutant with *p*-nitrophenyl phosphate compared with the nucleotide substrates can be rationalized by the fact that the pK_a of *p*-nitrophenol (7.2) is ~7 pH units lower than that of the 2′-OH and 3′-OH leaving groups of 2′-AMP and 3′-AMP. Previous studies from this laboratory have shown that severe defects incurred by alanine mutations of a general acid catalyst of phosphoryl transfer reactions of DNA topoisomerase IB can be alleviated by simple chemical substitutions in the substrate that lower the pK_a of the leaving group (Krogh and Shuman 2000, 2002). Whereas the substrate-specific effects of the *Cth*Pnkp H264A mutation are consistent with a mechanism of general acid catalysis, the findings that the H264N change restores activity with 2′-AMP and 3′-AMP substrates and significantly stimulates activity with *p*-nitrophenyl phosphate (Table 1) complicate the story. As mentioned above, the fact that asparagine but not glutamine is beneficial is inconsistent with a model whereby the gain of function is imparted by restoring a direct hydrogen bond between the amide group and the leaving phosphate oxygen. Rather, we propose that asparagine-264 is able to coordinate a water molecule, which in turn donates a proton to the leaving group. This scenario preserves the requirement for proton donation to expel the leaving group when its pK_a is high but allows for use of either a protein side chain as a general acid or an ordered water molecule as a specific acid.

The plasticity of the *Cth*Pnkp active site in accommodating asparagine instead of His264 contrasts with the intolerance of λ phosphatase for asparagine in lieu of the corresponding His76 side chain (Zhuo et al. 1994; Mertz et al. 1997). The finding that the H76N mutant of λ phosphatase exerted quantitatively similar effects on activity with *p*-nitrophenyl phosphate (pK_a 7.2) and phenyl phosphate (pK_a 10) can be interpreted as signifying that the histidine is not required for protonation of the leaving group (Mertz et al. 1997), although it remains possible that the histidine does play a critical role as a general acid in reactions with phosphoprotein substrates that have leaving groups with much higher pK_a values (Rusnak and Mertz 2000). Members of the metallophosphoesterase family may differ in the dependence of their catalytic parameters on the pK_a of the leaving group (Schenk et al. 2005).

Asp236 of *Cth*Pnkp is equivalent to Asp52 of λ phosphatase, which contacts Nδ of the proposed histidine general acid. The Asp–His pair could comprise a potential proton relay to the leaving group. The fact that the D236A mutant retains activity with *p*-nitrophenyl phosphate is consistent with a role in leaving group expulsion. Our mutational analysis of *Cth*Pnkp shows that an asparagine suffices for activity with all substrates; i.e., hydrogen-bonding, rather than full proton transfer between the Asp and His, is the relevant factor for catalysis.

Arg237 of *Cth*Pnkp corresponds to Arg53 in λ phosphatase, which makes multiple contacts with the sulfate (phosphate) oxygens in the crystal structure, suggestive of a role in transition state stabilization (Voegtli et al. 2000). Consistent with this idea, mutating Arg53 to alanine in λ phosphatase results in a 10^{-3} decrement in Mn^{2+}-dependent hydrolysis of *p*-nitrophenyl phosphate with no effect on the K_m for *p*-nitrophenyl phosphate (Zhuo et al. 1994). The R237A mutation of *Cth*Pnkp affects activity with 2′-AMP and 3′-AMP but has relatively little impact on either

K_m or k_{cat} for hydrolysis of *p*-nitrophenyl phosphate, a finding that contrasts sharply with the result for λ phosphatase. It seems unlikely that the lack of requirement for Arg237 in hydrolysis of *p*-nitrophenyl phosphate is related to the pK_a of the leaving group, insofar as arginine is a less plausible candidate than is histidine as a proton donor, although we cannot completely exclude this possibility at present. The fact that there are no contacts between arginine or lysine residues and the phosphate of 5′-dAMP in the crystal structure of *Pfu*Mre11 (Hopfner et al. 2001) attests to the variability of the requirements for phosphate contacts above and beyond those provided by the two metals and the catalytic asparagine (Asn263 in *Cth*Pnkp). Indeed, the amino acid sequence of *Pfu*Mre11 lacks an arginine at the position corresponding to Arg237 and Arg53 of *Cth*Pnkp and λ phosphatase, respectively (Hopfner et al. 2001). If the essential role of the arginine is exerted via transition state stabilization, then the differential requirement for this residue might reflect differences in the nature of the transition state. For example, in an associative mechanism, the phosphorane transition state develops an additional negative charge compared with the ground state, in which case the arginine could help neutralize this extra charge. In a dissociative mechanism, the metaphosphate transition state has a net loss of one negative charge compared with the ground state, in which case electrostatic effects of the arginine contacts might not be as critical for catalysis. With this line of reasoning, we speculate that *Cth*Pnkp hydrolysis of *p*-nitrophenyl phosphate (where leaving group departure is potentially easier) might have relatively more dissociative character, while hydrolysis of 2′-AMP and 3′-AMP might have a more associative character. Kinetic studies have suggested that λ phosphatase catalyzes manganese-dependent hydrolysis of *p*-nitrophenyl phosphate via a dissociative transition state (Hoff et al. 1999). The fact that the R237Q change in *Cth*Pnkp restores activity, relative to the alanine mutant, with 3′-AMP (and *p*-nitrophenyl phosphate) (Table 1) but not with 2′-AMP hints that there may be additional mechanistic differences in the way the enzyme reacts with various nucleotide substrates.

A complete description of the mechanism of the *Cth*Pnkp phosphatase will hinge on obtaining atomic structures of the enzyme at various steps along the reaction pathway. The delineation here of an autonomous phosphatase domain fragment of the trifunctional *Cth*Pnkp protein will facilitate efforts toward structure determination via crystallography.

MATERIALS AND METHODS

Materials

2′-AMP, 3′-AMP, *p*-nitrophenyl phosphate, and *p*-nitrophenol were purchased from Sigma. Malachite green reagent was purchased from BIOMOL Research Laboratories.

Recombinant *Cth*Pnkp

Alanine substitution mutations were introduced into the pET16-*Cth*Pnkp expression plasmid by PCR using the two-stage overlap extension method (Martins and Shuman 2005). N-terminal truncation alleles *CthPnkp*-(125–870), *CthPnkp*-(159–870), and *CthPnkp*-(171–870) were generated by PCR amplification using sense primers that introduced an NdeI site and a methionine codon in lieu of the codons for Gln124, Pro158, or Pro170. The C-terminal truncation alleles *CthPnkp*-(159–472), *CthPnkp*-(159–444), *CthPnkp*-(159–424), *CthPnkp*-(171–472), *CthPnkp*-(171–444), and *CthPnkp*-(171–424) were constructed by PCR amplification using an antisense primer that introduced a stop codon in lieu of the codons for Ile473, Ile445, or Lys425. All plasmid inserts were sequenced to confirm the presence of the intended mutations and verify that no other coding changes had been introduced during amplification and cloning. Wild-type and mutant pET16-*Cth*Pnkp plasmids were transformed into *E. coli* BL21(DE3). Cultures (500 mL) were induced to express *Cth*Pnkp as described previously (Martins and Shuman 2005); the recombinant His_{10}-tagged *Cth*Pnkp proteins were purified from soluble bacterial extracts by Ni-agarose affinity chromatography (Martins and Shuman 2005).

Nucleotide 2′, 3′ phosphatase assay

Phosphate release was measured colorimetrically by using the malachite green method (Lanzetta et al. 1979). Reaction mixtures (25 μL) containing 50 mM Tris-HCl (pH 7.5), 5 mM 2′-AMP or 3′-AMP, 5 mM $NiCl_2$, and *Cth*Pnkp as specified were incubated for 30 min at 45°C. The reactions were quenched by adding 1 mL of malachite green reagent. Release of phosphate was determined by measuring A_{620} and interpolating the value to a phosphate standard curve.

Hydrolysis of *p*-nitrophenyl phosphate

Reaction mixtures (25 μL) containing 50 mM Tris-HCl (pH 7.5), 10 mM *p*-nitrophenyl phosphate, 10 mM $NiCl_2$, and *Cth*Pnkp as specified were incubated for 30 min at 45°C. The reactions were quenched by adding 0.9 ml of 1 M Na_2CO_3. Release of *p*-nitrophenol was determined by measuring A_{410} and interpolating the value to a *p*-nitrophenol standard curve.

ACKNOWLEDGMENTS

This work was supported by NIH grant GM42498. S.S. is an American Cancer Society Research Professor.

Received August 16, 2005; accepted September 30, 2005.

REFERENCES

Amitsur, M., Levitz, R., and Kaufman, G. 1987. Bacteriophage T4 anticodon nuclease, polynucleotide kinase, and RNA ligase reprocess the host lysine tRNA. *EMBO J.* **6:** 2499–2503.

Bernstein, N.K., Williams, R.S., Rakovszky, M.L., Cui, D., Green, R., Karimi-Busheri, F., Mani, R.S., Galicia, S., Koch, C.A., Cass, C.E., et al. 2005. The molecular architecture of the mammalian DNA repair enzyme, polynucleotide kinase. *Mol. Cell* **17:** 657–670.

Blondal, T., Hjorleifsdottir, S., Aevarsson, A., Fridjonsson, O.H., Skirnisdottir, S., Wheat, J.O., Hermannsdottir, A.G., Hreggvidsson,

G.O., Smith, A.V., and Kristjansson, J.K. 2005. Characterization of a 5′-polynucleotide kinase/3′-phosphatase from bacteriophage RM378. *J. Biol. Chem.* **280:** 5188–5194.

Cameron, V. and Uhlenbeck, O.C. 1977. 3′-Phosphatase activity in T4 polynucleotide kinase. *Biochemistry* **16:** 5120–5126.

Chen, S., Yakunin, A.F., Kuznetsova, E., Busso, D., Pufan, R., Proudfoot, M., Kim, R., and Kim, S.H. 2004. Structural and functional characterization of a novel phosphodiesterase from *Methanococcus janaschii*. *J. Biol. Chem.* **279:** 31854–31862.

Galburt, E.A., Pelletier, J., Wilson, G., and Stoddard, B.L. 2002. Structure of a tRNA repair enzyme and molecular biology workhorse: T4 polynucleotide kinase. *Structure* **10:** 1249–1260.

Goldberg, J., Huang, H., Kwon, Y., Greengard, P., Nairn, A.C., and Kuriyan, J. 1995. Three-dimensional structure of the catalytic subunit of protein serine/threonine phosphatase-1. *Nature* **376:** 745–753.

Hoff, R.H., Mertz, P., Rusnak, F., and Hengge, A.C. 1999. The transition state of the phosphoryl transfer reaction catalyzed by the λ Ser/Thr protein phosphatase. *J. Am. Chem. Soc.* **121:** 6382–6390.

Hopfner, K.P., Karcher, A., Craig, L., Woo, T.T., Carney, J.P., and Tainer, J.A. 2001. Structural biochemistry and interaction architecture of the DNA double-strand break repair Mre11 nuclease and Rad50-ATPase. *Cell* **105:** 473–485.

Krogh, B.O. and Shuman, S. 2000. Catalytic mechanism of DNA topoisomerase IB. *Mol. Cell* **5:** 1035–1041.

———. 2002. Proton relay mechanism of general acid catalysis by DNA topoisomerase IB. *J. Biol. Chem.* **277:** 5711–5714.

Lanzetta, P.A., Alvarez, L.J., Reinach, P.S., and Candia, O.A. 1979. An improved assay for nanomole amounts of inorganic phosphate. *Anal. Biochem.* **100:** 95–97.

Martins, A. and Shuman, S. 2004. Characterization of a baculovirus enzyme with RNA ligase, polynucleotide 5′ kinase and polynucleotide 3′ phosphatase activities *J. Biol. Chem.* **279:** 18220–18231.

———. 2005. An end-healing enzyme from *Clostridium thermocellum* with 5′ kinase, 2′,3′ phosphatase, and adenylyltransferase activities. *RNA* **11:** 1271–1280.

Mertz, P., Yu, L., Sikkink, R., and Rusnak, F. 1997. Kinetic and spectroscopic analysis of mutants of a conserved histidine in the metallophoshatases calcineurin and λ protein phosphatase. *J. Biol. Chem.* **272:** 21296–21302.

Mueller, E.G., Crowder, M.W., Averill, B.A., and Knowles, J.R. 1993. Purple acid phosphatase: a diiron enzyme that catalyzes a direct phospho group transfer to water. *J. Am. Chem. Soc.* **115:** 2974–2975.

Novogrodsky, A. and Hurwitz, J. 1966. The enzymatic phosphorylation of ribonucleic acid and deoxyribonucleic acid: Phosphorylation at 5′-hydroxyl termini. *J. Biol. Chem.* **241:** 2923–2932.

Novogrodsky, A., Tal., M., Traub, A., and Hurwitz, J. 1966. The enzymatic phosphorylation of ribonucleic acid and deoxyribonucleic acid: Further properties of the 5′-hydroxyl polynucleotide kinase. *J. Biol. Chem.* **241:** 2933–2943.

Richardson, C.C. 1965. Phosphorylation of nucleic acid by an enzyme from T4 bacteriophage-infected *Escherichia coli*. *Proc. Natl. Acad. Sci.* **54:** 158–165.

Rusnak, F. and Mertz, P. 2000. Calcineurin: Form and function. *Physiol. Rev.* **80:** 1483–1521.

Schenk, G., Gahan, L.R., Carrington, L.E., Mitic, N., Valizadeh, M., Hamilton, S.E., de Jersey, J., and Guddat, L.W. 2005. Phosphate forms an unusual tripodal complex with the Fe-Mn center of sweet potato purple acid phosphatase. *Proc. Natl. Acad. Sci.* **102:** 273–278.

Voegtli, W.C., White, D.J., Reiter, N.J., Rusnak, F., and Rosenzweig, A.C. 2000. Structure of the bacteriophage λ Ser/Thr protein phosphatase with sulfate ion bound in two coordination modes. *Biochemistry* **39:** 15365–15374.

Wang, L.K. and Shuman, S. 2001. Domain structure and mutational analysis of T4 polynucleotide kinase. *J. Biol. Chem.* **276:** 26868–26874.

———. 2002. Mutational analysis defines the 5′-kinase and 3′-phosphatase active sites of T4 polynucleotide kinase. *Nucleic Acids. Res.* **30:** 1073–1080.

Wang, L.K., Lima, C.D., and Shuman, S. 2002. Structure and mechanism of T4 polynucleotide kinase: An RNA repair enzyme. *EMBO J.* **21:** 3873–3880.

White, D.J., Reiter, N.J., Sikkink, R.A., Yu, L., and Rusnak, F. 2001. Identification of the high affinity Mn^{2+} binding site of bacteriophage λ phosphoprotein phosphatase: Effects of metal ligand mutations on electron paramagnetic resonance spectra and phosphatase activities. *Biochemistry* **40:** 8918–8929.

Zhu, H., Yin, S., and Shuman, S. 2004. Characterization of polynucleotide kinase/phosphatase enzymes from mycobacteriophages Omega and Cjw1 and vibriophage KVP40. *J. Biol. Chem.* **279:** 26358–26369.

Zhuo, S., Clemens, J.C., Hakes, D.J., Barford, D., and Dixon, J.E. 1993. Expression, purification, crystallization, and biochemical characterization of a recombinant protein phosphatase. *J. Biol. Chem.* **268:** 17754–17761.

Zhuo, S., Clemens, J.C., Stone, R.L., and Dixon, J.E. 1994. Mutational analysis of a Ser/Thr phosphatase: Identification of residues important in phosphoesterase substrate binding and catalysis. *J. Biol. Chem.* **269:** 26234–26238.